Soft Matter

Accepted Manuscript

ROYAL SOCIETY OF CHEMISTRY

www.rsc.org/softmatter

Journal Name

RSCPublishing

ARTICLE

Two glass transition behaviour of polyurea networks: effect of the segmental molecular weight

Cite this: DOI: 10.1039/x0xx00000x

Received 00th January 2012,
Accepted 00th January 2012

DOI: 10.1039/x0xx00000x

www.rsc.org/

Marius Reinecker,*[a] Viktor Soprunyuk,[a] Martin Fally,[a] Antoni Sánchez-Ferrer *[b] and Wilfried Schranz *[a]

Polymer-nanoparticle composites (PNCs) play an increasing role in technology. Inorganic or organic nanoparticles are usually incorporated into a polymer matrix to improve material properties. Polyurea is a spontaneously occurring PNC, exhibiting a phase segregated structure with hard nanodomains embedded in a soft (elastically compliant) matrix. This system shows two glass transitions at T_{g1} and T_{g2}. It has been argued that they are related to the freezing of motion of molecular segments in the soft matrix (usual polymer α–glass transition at T_{g1}) and to regions of restricted mobility near the hard nanodomains (α´-process) at T_{g2}, respectively.
We present detailed dynamic mechanical analysis (DMA) measurements for polyurea networks with different segmental lengths l_c (2.5, 12.1, 24.5 nm) of the polymer chains, i.e. different volume fractions ϕ_x (0.39, 0.12, 0.07) of the hard domains. The two glass transitions show up in two distinct peaks in tanδ at T_α and $T_{\alpha'}$. Analysing the data using a Havriliak-Negami term for the α- and the α´- relaxation, as well as Vogel-Fulcher dependencies for the corresponding relaxations times, it is found, that the α-glass transition at T_{g1} increases strongly (up to ΔT=70 K) with increasing ϕ_x, whereas the α´-transition at T_{g2} remains unchanged. At $\phi_x^c \approx 0.19$ the two curves intersect, i.e. $T_{g1} = T_{g2}$. This value of ϕ_x^c is very close to the percolation threshold of randomly oriented overlapping ellipsoids of revolution with an aspect ratio of about 1:4 - 1:5. We therefore conclude, that around 19% of hard nanodomains polyurea changes from a system of hard nanoparticles embedded in a soft matrix ($\phi_x \leq \phi_x^c$) to a system of soft domains confined in a network of percolated hard domains at $\phi_x \geq \phi_x^c$.

I Introduction

The glass transition remains one of the great mysteries in material science despite of decades of intense research. According to the work of Adam and Gibbs [1] the generally observed drastic slowing down of the dynamics around T_g originates from so called "cooperatively rearranging regions (CRRs)", whose size ξ increases when T approaches T_g. The corresponding relaxation time $\tau_\alpha(\xi)$ is given by [2]

$$\tau_\alpha(\xi) = \tau_0 exp\left[\xi(T)^D \frac{\Delta}{k_B T}\right] \quad (1)$$

Where Δ is a typical energy scale that depends on the details of the glass former and is traditionally assumed to be constant. ξ(T) contains the main T dependence and *D* is the spatial dimension of correlated regions. The glass transition temperature T_g (so called "laboratory glass transition temperature") is usually defined for $\tau_\alpha \approx 100$ s or shear viscosities in the range of about 10^{13} poise. [3] The main question, whether there is a true thermodynamic phase below T_g, or if it is just a kinetic slowing down at T=0 K, is intimately related to the question of a diverging correlation length ξ at a finite temperature T_0 below T_g. Substantial progress has been made in recent years to determine such length scales. Quite different experimental techniques, such as heat capacity spectroscopy,[4] multidimensional NMR,[5,6] dielectric spectroscopy[7] as well as computer simulations[8] have been used to monitor a possible growing length scale accompanying the glass transition in various glass forming materials including molecular liquids and polymers.
It is now generally accepted, that the nature of cooperativity is dynamic and the obtained dynamically correlated regions ξ are increasing when approaching T_g. However, it is very difficult to nail down quantitative values for ξ exactly. To a great extent this is due

to the unknown shape of correlated regions, which can change from compact to string like structures with changing temperature.[8,9]

An appealing method to probe correlation lengths in glass forming materials is to restrict their spatial extent *d*. The basic idea is the following: If a growing correlation length $\xi(T)$ for $T \rightarrow T_g$ would be involved in the glass transition, the system should start to "feel" the spatial confinement as soon as $\xi(T_g) \approx d$, and the glass transitions should be finally suppressed for $d < \xi(T_g)$. Indeed, numerous measurements of confined glass forming materials, i.e. of thin polymer films,[10,11] molecular liquids in nanopores,[12,13,14] as well as computer simulations[15,16] support this idea. In most cases confinement leads to a remarkable downshift of T_g, due to so called "confinement induced acceleration of the dynamics". There are however also cases, where a gradual increase of the glass transition temperature with decreasing pore size was reported.[17] It turns out that attractive interactions between the confined glass former and the pore surface can slow down the motion of molecules near the surface, which due to an increase in correlation length can slow down larger regions, leading to an effective upshift of T_g. Interestingly it was found, [18,19] that a second glass transition at $T_{g2}>T_g$ can occur if the interfacial region of slowed down motion is large enough, i.e. of the order of the correlation volume $V_{corr}(T_g)$ of dynamically correlated regions. Effects of confinement on material behaviour including freezing and melting have been discussed in excellent review articles.[20,21]

Exciting interfacial phenomena have been also studied by incorporation of nanoparticles into a polymer host.[22] Depending on the type of interaction (attractive or repulsive) between the polymer chains and the nanoparticles, the relaxation dynamics of the polymer chains close to the nanoparticles may increase (for repulsive interactions) or decrease (for attractive interactions), leading to a down- or upshift of T_g, respectively.[23,24] In case of permanent attachment of polymer chains to nanoparticles one can even obtain two glass transitions : [25] one at T_{g1} associated with polymer chains far from the nanoparticles and a second $T_{g2}>T_{g1}$ associated with chain segments in the vicinity of the nanoparticles. Indeed such polymer nanocomposites (PNCs) are in many respects similar to confined pure polymers or liquid glass formers in nanopores.[26]

Polyurea is a unique material, [27] since it offers the possibility to study the influence of nanoparticles to the glass dynamics without the need to add nanoparticles due to its microphase segregated structure into hard and soft nanodomains, whose volume ratios can be easily varied by changing the molecular weight of the polyetheramines. The type of interaction (attractive vs. repulsive) between the polymer chains near the hard nanodomains is clearly attractive, since the polymer chains are chemically attached to the hard nanodomains. Due to the complex microstructure polyureas display a very broad range of mechanical responses under static and dynamic loading conditions, which favour their use as abrasion/corrosion protection and blast/ballistic-impact mitigation material.

In the present work we use samples of polyurea networks with three different segmental lengths l_c (Table 1) of the polymer backbone (i.e. polyetheramine in our case) resulting in three different volume fractions ϕ_x of the hard nanodomains and perform dynamic mechanical analysis measurements (DMA) as a function of temperature and frequency. Two successive glass transition temperatures at T_{g1} and T_{g2} are found and are attributed to cooperative motions of molecular segments in the soft matrix (T_{g1}) and to regions in the vicinity of the hard domains (T_{g2}), respectively.

Fitting a Havriliak-Negami function with the Vogel-Fulcher relaxation time behaviour to the temperature and frequency dependence of the experimental tanδ - curves, we determine the glass transition temperatures $T_{g1}(\phi_x)$ and $T_{g2}(\phi_x)$ for various concentrations ϕ_x of hard nanodomains.

From the experimental data of the Young´s modulus vs. temperature and frequency $E'(\omega,T)$ we determine the temperature dependence of the linear size ξ and volume V_{corr} of dynamically correlated regions using the multipoint susceptibility approach of Berthier, *et al.* [7] We show that these obtained values are consistent with the hypothesis [25] that the regions of restricted mobility near the hard domains have to exceed a critical size of the order of $V_{corr}(T_g)$ to exhibit their own glass transition at T_{g2}. Moreover, the obtained values of $\xi(T)$ turn out to be large enough to explain the observed increase of T_{g1} with increasing volume fraction of hard nanodomains.

II Experimental

A Samples

For the present study, the three linear hydrophobic diamino-terminated polyetheramines Jeffamine D-400 (M_n = 460 g·mol^{-1}, ρ = 972 kg·m^{-3}), D-2000 (M_n = 2060 g·mol^{-1}, ρ = 991 kg·m^{-3}) and D-4000 (M_n = 4000 g·mol^{-1}, ρ = 994 kg·m^{-3}) from Huntsman International LLC, and the triisocyanate crosslinker Basonat HI-100 (m_w= 504 g·mol^{-1}, ρ = 1174 kg·m^{-3}) from BASF SE, were used as received. Polyurea (PU) networks are formed by the rapid chemical reaction between a triisocyanate and a diamine to build urea moieties, as shown in Fig. 1. Details of the synthesis of these PU elastomers are well described in the literature.[27] Table 1 compares the main structural characteristics for the three used samples JD-400, JD-2000 and JD-4000.

Table 1 Segmental molecular weight ($\bar{M}_c$) of polyetheramines, segmental length (l_c), volume fractions (ϕ_x) of the crosslinker (hard domains) and average distance t between hard domains for all three polyurea elastomers.

Sample	$\bar{M}_c$ (g/mol)	l_c (nm)	ϕ_x	t (nm)
JD-400	428	2.5	0.39	4.8
JD-2000	1990	12.1	0.12	5.4
JD-4000	4024	24.5	0.07	7.5

The structure of polyurea chains is shown in Fig. 1 (top). **U-R-U** represents the hard segment **(HS)** of the polyurea

molecule and **R´** the soft segment (**SS**), and thus we can represent the molecules as shown in the bottom of Fig. 1.

Due to strong hydrogen bonding between urea linkages of neighboring chains or neighboring segments in the same chain, hard segments (HS) are usually microphase segregated into so called "hard domains".

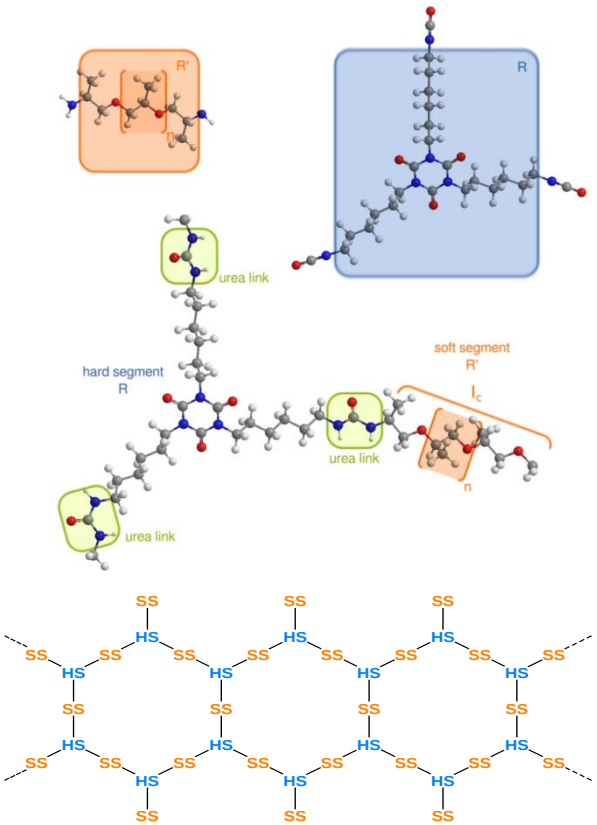

Figure 1 Representation of a typical polyurea chain (top). R represents triisocyanate crosslinker Basonat and R´ denotes the diamino-terminated polyetheramine Jeffamine. The sketch at the bottom shows polyurea molecules built of hard and soft segments.

Atomic force microcopy [28] investigations revealed islands of hard domains embedded in the soft matrix where the average distance between hard domains is of the order of several nm (Table 1).

For small volume fractions of hard nanodomains the topology of phase segregated polyurea is "inverse" to the case of molecular liquids confined in meso- or nano-porous silica frameworks like Vycor or Gelsil. In these systems we recently studied the glass transitions of various glass forming liquids with varying pore diameters. [29,30] E.g. for salol confined in nanoporous silica we detected [29] two glass transitions for pore sizes larger than 5 nm. We could associate the glass transition at $T_{g2}>T_{g1}$ with regions of restricted mobility near the surface of the pores. The glass transition at T_{g1} was attributed to regions well inside the pores. Its dynamics was however also slowed down by surface interactions. This could be proved by silanization of the pore surface: removing the surface interactions resulted in a stronger decrease (as compared to untreated pores) of the bulk glass transition T_{g1} with decreasing pore size and the second glass transition at T_{g2} disappeared.[30]

In polyurea one obtains the inverse geometrical case for small enough volume fractions ϕ_x of hard domains, as the elastically hard domains are suspended in the elastically compliant (soft) matrix. However, with increasing ϕ_x we can expect a crossover to a system that is very similar to the case of glass forming liquids in nanopores.

B Experimental methods

Dynamic mechanical analysis (DMA) is used to measure the temperature dependencies of the low frequency elastic moduli and damping of polyurea at frequencies between 0.1 and 100 Hz. A static force F_{stat} is sinusoidally modulated by a dynamic force $F_{dyn}\sin(\omega t)$ at a chosen amplitude and frequency. The elastic and anelastic response of the sample leads to a change in length u and phase shift δ between force and response amplitude with resolutions for the length and phase shift of $\Delta u\approx 10$ nm and $\Delta\delta\approx 0.1°$, respectively. The knowledge of the sample length u and the phase shift δ allows to determine the real and imaginary parts of a certain component of the complex elastic compliance tensor S_{ii}^*

$$S_{ii}' = S_{ii}\cos\delta \quad \text{and} \quad S_{ii}'' = S_{ii}\sin\delta \qquad (2)$$

The corresponding storage (E´) and loss modulus (E´´) are defined as $E':=1/S_{ii}'$ and $E'':=1/S_{ii}''$, respectively and $\tan\delta=E''/E'$.

DMA experiments are performed on a Perkin Elmer Diamond DMA. The complex elastic compliance can be measured in a frequency range between 0.1 Hz and 100 Hz, and for temperatures between 80 K and 850 K. The minimal (maximal) force that can be applied is 10^{-3} N (10 N) with a resolution of 10^{-5} N. It is transmitted via a steel-rod. The present experiments are performed in tensile stress geometry (Fig.2). For more details concerning the DMA method see e.g. Ref [31]. Typical sample size was $9 \times 2 \times 0.2$ mm^3. The samples were cooled down to about 90 K and heated again with a heating rate between 0.5 and 2 K/min. Up to 5 heating/cooling cycles were performed for each measurement frequency and each sample.

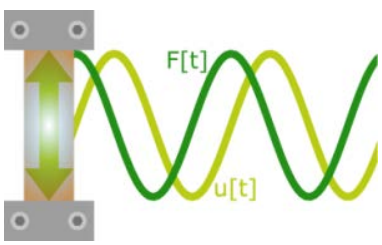

Figure 2 Sketch of DMA measurement in tensile stress geometry.

III Experimental results

Fig. 3 shows the storage modulus E´and tanδ of JD-2000 as a function of temperature at various frequencies.

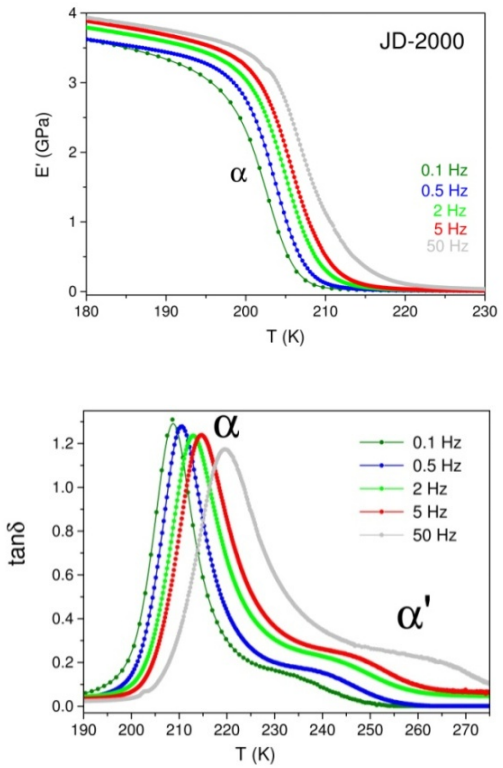

Figure 3 Temperature dependence of storage modulus E´ and tanδ of polyurea JD-2000 at various frequencies.

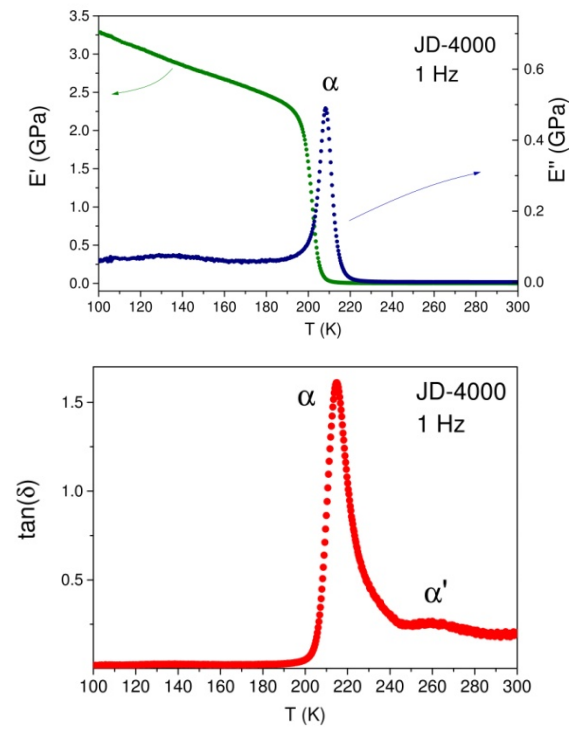

Figure 4 Temperature dependence of storage modulus E´, loss modulus E´´ and tanδ of polyurea JD-4000 measured at f=1Hz.

In Fig. 4 and Fig. 5 the same quantities are plotted for JD-4000 and JD-400, respectively for f=1Hz.

Inspecting Figures 3-5 one recognizes quite similar behaviour for JD-2000 and JD-4000 samples. A typical relaxation behaviour of E´(ω,T) together with the corresponding peak(s) in tanδ whose maximum shifts to higher temperatures with increasing frequency. In JD-2000 and JD-4000 a second peak (α') is observed in tanδ (Fig. 3 and 4). It can be seen in E´´ data only if the scale is increased. The underlying process of this α'-relaxation will be discussed in detail below. Note, that there is only a single broad tanδ-peak in JD-400 (Fig. 5).

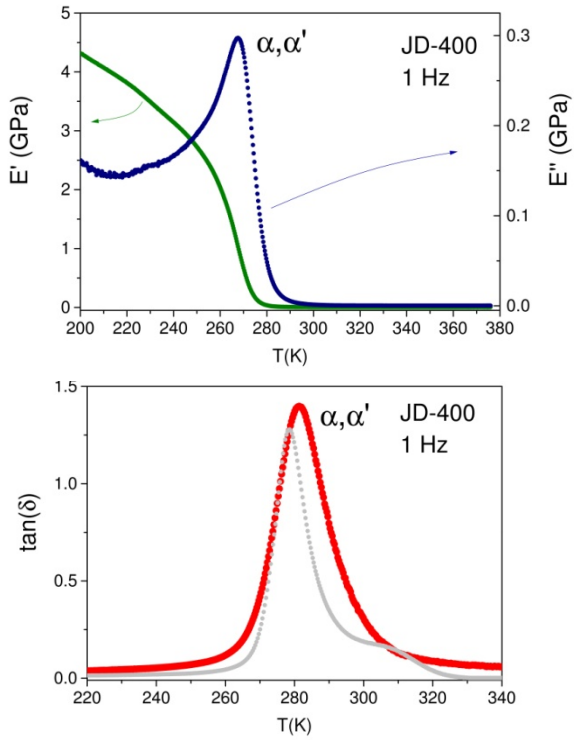

Figure 5 Temperature dependence of storage modulus E´, loss modulus E´´ and tanδ of polyurea JD-400 (red disks) measured at f=1Hz. The grey disks display the shifted (with respect to T) tanδ of JD-2000 (at 0.5 Hz) for comparison to emphasize the broadness of the JD-400 peak.

In all samples we observed also two additional peaks at lower temperatures, often denoted as β– and γ– relaxations. They are related to motions of side groups and other local molecular motions and have been also observed in previous DMA measurements of polyurea. [32] As we focus on the α- and α'-process here we will show these details in a forthcoming paper.

IV Discussion

The segmental dynamics of polyurea was already previously studied by dynamic mechanical analysis [32,33] as well as by dielectric spectroscopy. [34] Contrary to these DMA [32,33] and

specific heat [34] measurements our DMA data clearly show (in tanδ of JD-2000 and JD-4000) a second relaxation process (α') at a temperature higher than the α-peak (Fig. 3 and Fig. 4). As we shall show below, for JD-400 (Fig. 5) the two glass transitions can only be separated by a careful fitting procedure.

In dielectric spectroscopy measurements [34] a similar second relaxation process was found (denoted there also as α´-process) and turned out to be about 3 orders of magnitude slower than the α – relaxation. Calorimetric data show [34], that the α- transition in polyurea is very broad with a ΔT ≈ 30 - 35 K. This indicates a rather heterogeneous dynamics. Such a broad distribution of relaxation times can be accounted for by fitting a double Havriliak-Negami [35] term for the α- and the α´-relaxation to the data

$$E^*(\omega) = E_\infty - \sum_{j=1}^{2} \frac{\Delta E_j}{\left[1+(i\omega\tau_j)^{\alpha_j}\right]^{\beta_j}} \qquad (3)$$

where j=1,2 correspond to the α- and α'-relaxation, respectively. E_∞ is the unrelaxed (high frequency limit) Young´s modulus, $\Delta E_1 = E_\infty - E_{s1}$ and $\Delta E_2 = E_{s1} - E_{s2}$ (E_{s1} and E_{s2} are the static moduli of the corresponding process). The exponents α_j and β_j describe the broadness and asymmetry of the corresponding spectra.

The temperature dependencies of the two relaxation times τ_j can be written in terms of Vogel-Fulcher relations as [36]

$$\tau_j = \tau_{0j} exp\left(\frac{B_j}{T - T_{0j}}\right) \qquad (4)$$

where τ_{0j} describe attempt rates, B_j the activation energies and T_{0j} the corresponding Vogel-Fulcher temperatures of the α- and α'-process, respectively.

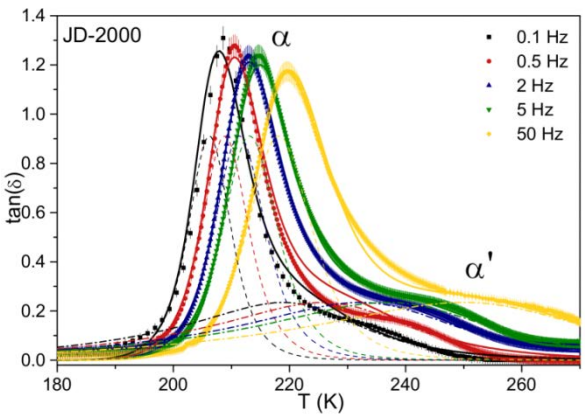

Figure 6 Measured temperature dependence of tanδ of polyurea JD-2000 (disks). The full lines show a simultaneous fit for all measured frequencies with Eqs. (3) and (4). Dotted lines are generated by considering either the α- or the α´-relaxation.

Fig. 6, 7 and 8 show fits of tanδ to the corresponding data of JD-2000, JD-4000 and JD-400 using Eq.(3) and Eq.(4). The resulting fitting parameters are displayed in Table 2.

Contrary to JD-2000 and JD-4000 the tanδ curve of JD-400 exhibits only a single peak (Fig. 8), and hence does not obviously display two relaxation processes. However, it is impossible to fit the data assuming a single relaxation process in Eq.(3). On the other hand we cannot uniquely separate the α and α´- contributions. Therefore we varied the relaxation contributions ΔE_1 and ΔE_2 in Eq.(3), resulting in fits of similar quality characterized by chi-square values ranging from 0.28 to 0.39. However, while T_{g1} is determined with high accuracy the uncertainty of T_{g2} is ± 10.6 K.

Taking into account, that mechanically measured relaxation times are usually shorter than dielectrically determined ones [37] the fitting parameters in Table 2 are in reasonable agreement with those determined from dielectric spectroscopy data.[34] Moreover, the main fitting parameters for the polyureas with different hard/soft segment ratios turn out to be rather similar.

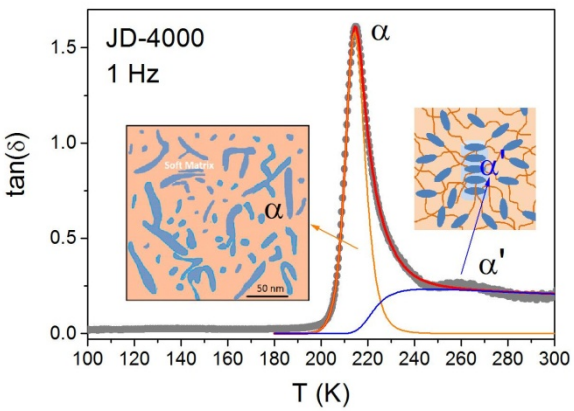

Figure 7 Measured temperature dependence of tanδ of polyurea JD-4000 (grey disks). The red full line shows a fit with Eqs. (3) and (4). Orange and blue lines are generated by considering either the α- or the α´-relaxation. The inset sketches the spatial regions of α and α' relaxations.

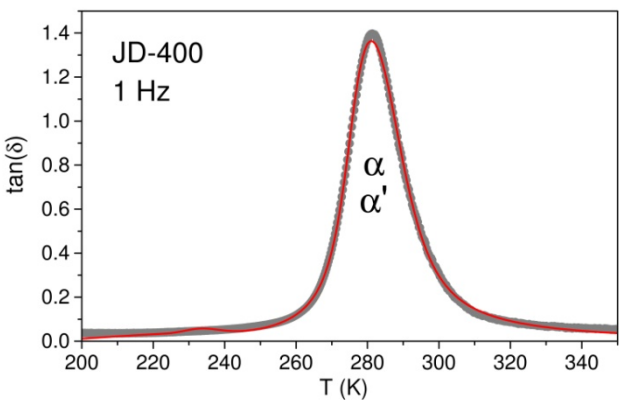

Figure 8 Measured temperature dependence of tanδ of polyurea JD-400 (grey disks). The red line shows a fit with Eqs. (3) and (4). Here we

do not show separate curves, since we cannot uniquely disentangle the α and α´- contributions.

Table 2 α and α' relaxation parameters for the three polyureas JD-4000, JD-2000 and JD-400 obtained from fits with Eq. (3) and Eq.(4).

	JD-4000	JD-2000	JD-400
T_{01} (K)	156.6	153.8	221.5
α1	0.78	0.7	0.66
β1	0.48	0.39	0.001
τ_{01}(s)	10^{-15}	10^{-15}	10^{-15}
B_1 (K)	1755	1755	1755.2
$\Delta E_1/E_\infty$	0.99	0.97	0.7
T_{02}(K)	206.3	92	171.8
α2	0.16	0.57	0.61
β2	0.36	0.098	0.17
τ_{02}(s)	10^{-13}	10^{-13}	10^{-13}
B_2 (K)	565.7	4010	1388
$\Delta E_2/E_\infty$	0.0099	0.026	0.299

In the following we will calculate the temperature dependence of dynamically correlated regions when approaching the glass transition in polyurea JD-2000 using the multipoint susceptibility approach of Ref. 7. In their work the authors proposed a very general but straightforward method to calculate a number of dynamically correlated units - which they call $N_{corr,4}(T)$ - in glass forming materials. Relating un-measurable four-point correlations to an easily accessible response function, e.g. the temperature derivative of a dynamic two-point correlation function they obtain [38]

$$N_{corr,4}(T) = \frac{k_B N_A}{\Delta C_P \bar{M}_C} T^2 \{\max_\omega \chi_T(\omega, T)\}^2 \qquad (5)$$

where ΔC_P [$Jg^{-1}K^{-1}$] is the specific heat anomaly at the glass transition temperature, N_A the Avogadro constant, $\bar{M}_c$ the segmental molecular weight of the polyetheramines (soft segments) and $\chi_T(\omega,T)=(1/E_\infty)dE´(\omega,T)/dT$ is the temperature derivative of a suitable correlation function (here the real part of the complex Young´s modulus E´ normalized with respect to E_∞). In these units we obtain $N_{corr,4}$ in terms of the number of correlated soft segments. To calculate an appropriate length scale ξ we then have to multiply $N_{corr,4}$ by the corresponding segmental length l_c (Table 1).

Fig. 9 shows the temperature derivatives of the Young´s modulus of JD-2000 as a function of frequency for various temperatures near the α-glass transition. From the corresponding maxima, we have calculated $N_{corr,4}(T)$, which is increasing with decreasing temperature. Values of $N_{corr,4}$ for many glass forming materials are reported in the literature, [2,7,38] and it was shown that this quantity indeed increases when approaching T_g, implying that dynamical correlations increase when approaching the glass transition.

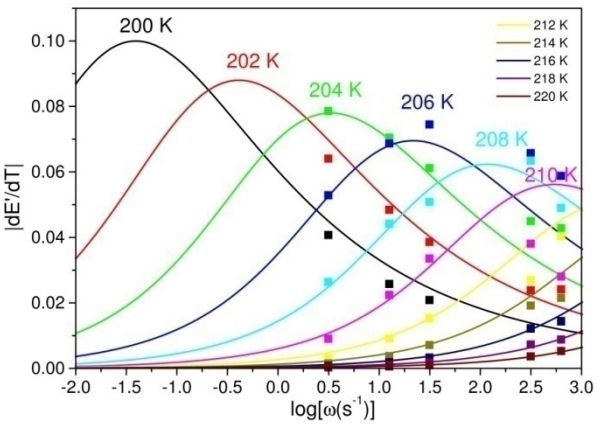

Figure 9 Temperature derivatives of normalized Young´s moduli as function of frequency for various temperatures. Points are from experimental data of JD-2000 (Fig. 3) and lines are calculated from the corresponding fits to E'(ω,T).

It is nontrivial to relate the value of $N_{corr,4}$ to certain values of spatially correlated regions. This is due to the fact, that there is no need for the associated correlation volume V_{corr} to be compact and therefore to scale as $V_{corr} = N_{corr,4}/\rho \sim\xi^3$ as is the case for isotropic correlations. Although some theories, like e.g. the random first-order transition theory (RFOT) of glasses predicts that these correlated regions are compact, computer simulations suggest that CRRs are string-like. [8,9,39]

To get a reliable estimation of the spatial correlations in polyurea we proceed as follows. Exploiting the approach described above, we calculate $N_{corr,4}(T)$ (with [34] ΔC_P=0.5 $JK^{-1}g^{-1}$) and further the correlation volume $V_{corr}(T)$ (Fig. 10). At the laboratory glass transition T_{g1}=198.6 K, defined as $\tau_1(T_{g1})$=100 s, we obtain $V_{corr}(T_{g1})\approx$10.2 nm^3. Assuming a compact correlation volume and isotropic correlations this would imply $\xi\approx V_{corr}^{1/3}$, leading to $\xi(T_{g1})\approx$2 nm. If however, we assume the dynamic correlations in polyurea to be string-like we can estimate their approximate length scale following two different approaches, which turn out to yield almost identical results (Fig. 10). For the first one, we assume that cylindrically shaped strings have an approximate thickness of a polyurea molecule [40], i.e.2r ≈ 0.56 nm – with $\xi = V_{corr}/(r^2\pi)$ – this leads to the blue disks in Fig. 10. For the second approach we calculate ξ(T) (green disks in Fig. 10) from the number of correlated segments $N_{corr,4}$ using Eq.(5) with the corresponding segmental length (l_c=12.1 nm for JD-2000) of Table 1.

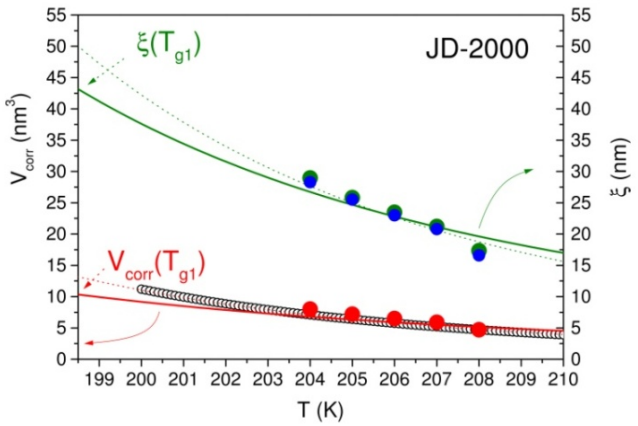

Figure 10 Temperature dependencies of dynamically correlated regions approaching the α-glass transition in polyurea JD-2000. The few full circles between 204 and 208 K are determined from the experimental values of E´(ω,T) using Eq.(5) together with $V_{corr}=N_{corr,4}/\rho$ (red disks), $\xi=V_{corr}/(r^2\pi)$ (blue) and $\xi=l_c N_{corr,4}$ (green disks) . The black open circles of V_{corr} are determined by extrapolating the experimental data of dE'/dT by the fitted ones to 200 K. The full lines are fits with Eq.(7) using the fitting parameters B_1 and T_{01} of Table 2. Dotted lines were obtained by varying the exponent in Eq.(7) from 4 to 5.3.

Fig. 10 shows the temperature dependencies of V_{corr} and ξ. The points represent the experimentally determined values using Eq.(5) and the procedures described above. The lines are fits using the relation [2,38]

$$V_{corr}(T) = \frac{N_{corr,4}(T)}{\rho} \propto \frac{k_B}{\rho \Delta C_P} T^2 \left(\frac{d \ln \tau}{dT}\right)^2 \qquad (6)$$

which by using the Vogel-Fulcher temperature dependence Eq.(4) for τ(T) Eq.(6) can be written as

$$V_{corr}(T) = \frac{N_{corr,4}(T)}{\rho} \propto \frac{k_B}{\rho \Delta C_P} T^2 \frac{B^2}{(T-T_0)^4} \qquad (7)$$

leading to $\xi(T_{g1})\approx 43$ nm.

After these data evaluations we arrive at the following picture for the two-glass transition behaviour of polyurea. For the α-process dynamical correlations between molecules are increasing with decreasing temperature (Fig. 10) leading to a collective slowing down of (most probably string-like) molecular motions in the soft matrix.

We argue that the α'-process is related to a freezing of the motion of soft segments of restricted mobility in the vicinity of the hard domains for the following reasons: Contrary to the α-transition, the α'-transition affects the real part of the complex Young´s modulus only very little (from Table 2 we obtain $\Delta E_2 \approx 0.027 \Delta E_1$), which is in agreement with the assumption, that the α'-transition takes place in a very small shell surrounding the hard domains (Fig. 7).

The size of the hard nanodomains is of the order of ≈ 3 – 4 nm. This nanodomain size was calculated taking into account the volume fraction of both hard and soft domains, the average distance between two hard nanodomains (Table 1) which was obtained from the maximum intensity peak in the SAXS region ($d = 2\pi/q$),[27] and the packing of spheres as an ideal model – primitive cubic (PC), body-centered cubic (BCC) and face-centered cubic (FCC). The estimated radius of this hard domains is proportional to the product of the lattice parameter times the square root of the volume fraction of the crosslinker ($r \propto a\ \phi_{HD}^{1/2}$); PC: $r = a[3\phi_{HD}/(4\pi)]^{1/2}$, BCC: $r = a[3\phi_{HD}/(8\pi)]^{1/2}$, and FCC: $r = a[3\phi_{HD}/(16\pi)]^{1/2}$. From the calculated areas of the tanδ peaks with respect to the α- and the α´-transition, we have estimated the thickness of the surrounding layer of restricted mobility to be of the order of λ≈0.2 nm for JD-2000 when considering a packing of such model spheres with a hard-to-hard domain distance of d = 5.4 nm and volume fraction of 0.04 and 0.84 for the polymer segment directly attached to the hard nanodomain interface and the bulk polymer, respectively.

The corresponding volume of this surrounding shell, which then is of the order of ≈30 nm^3, is larger than the correlation volume $V_{corr}(T_{g1})$ ≈10 nm^3 (Fig. 10). It implies that the region of restricted mobility is large enough to exhibit its own glass transition at T_{g2}. Similar estimations hold also for JD-4000 and for JD-400.

Using the fitting parameters (Table 2) one obtains (Fig. 11), that in the vicinity of the α'-peak the dynamics of these motions is indeed several orders of magnitude slower as compared to the dynamics of the polymer chain motions in the soft matrix (α–process).

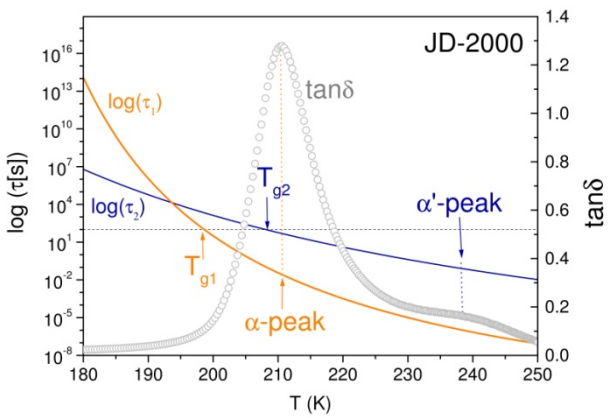

Figure 11 Temperature dependencies of relaxation times τ_1 and τ_2 for JD-2000 calculated from Eq.(4) with the parameters of Table 2. Tanδ was measured at 0.5 Hz.

Computer simulations [15,23,41] show, that the relaxations of chain segments in the vicinity of nanoparticles are necessarily slowed down, if there is an attractive interaction between nanoparticles and polymer chains. This is certainly the case here, since the soft segments (SS) are chemically attached to the hard domains. Under such conditions of permanent attachment PNCs have shown to exhibit two glass transition temperatures: [42] one associated with polymer chains in the soft matrix far from the

nanoparticles (hard domains in our case), and the other one at higher temperature is associated with chains in the vicinity of the nanoparticles (hard domains).
Table 3 gives the glass transition temperatures for the three polyureas obtained from the fitting parameters of Table 2.

Table 3 Glass transition temperatures calculated from fitting parameters of Table 2 using $\tau(T_g)$=100 s.

Sample	Tg_1 (K)	Tg_2 (K)
JD-400	266.3 ± 0.2	217.2 ± 10.6
JD-2000	198.6 ± 0.4	208.2 ± 2.1
JD-4000	201.4 ± 0.2	222 ± 1.4

Fig. 12 shows the dependencies of the glass transition temperatures on the volume fractions ϕ_x of the crosslinker (hard domains) and a fit with the relation [43]

$$T_{g1} = T_{g1}^0 + k\frac{\phi_x}{1-\phi_x} \quad (8)$$

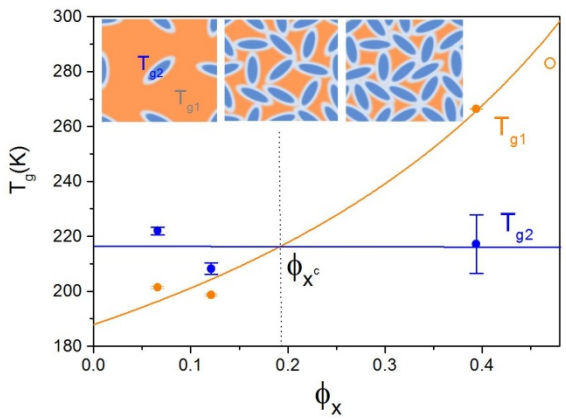

Figure 12 Glass transition temperatures of three polyurea networks JD-4000, JD-2000 and JD-400 vs. volume fractions ϕ_x of the hard nanodomains. The orange line is a fit with Eq. (8), yielding T_{g1}^0=(187.9 ± 6.6) K and k=(119.6 ± 17.2) K. The polyurea elastomer [27] ET-403 with a volume fraction of ϕ_x =0.47 (orange open circle) follows the trend rather well.

Inspecting Fig. 12 we observe, that around the critical volume fraction of $\phi_x^c \approx 0.19$ the two glass transitions reverse order, implying $T_{g1} = T_{g2}$ for ϕ_x^c. This value of 0.19 corresponds to the percolation threshold of randomly oriented overlapping ellipsoids[44] of revolution with an aspect ratio of about 1:4 – 1:5. It implies, that for ϕ_x less than 19% the system consists of hard nanodomains embedded in a soft matrix. At ϕ_x^c the hard nanodomains percolate. For $\phi_x > \phi_x^c$ the system consists of soft islands surrounded by a percolated network of hard nanodomains.
Finally we will discuss the physical origin of the strong increase of T_{g1} with increasing ϕ_x. Because the size ξ of CRRs increases for $T \rightarrow T_{g1}$ (Fig. 10), the molecules of polymer chains at distances $r \leq \xi$ away from the surface of the hard nanodomains will "feel" the surface induced slowing down. Since the average distance between the hard nanodomains is smaller than $\xi(T_{g1}) \approx 43$ nm, the dynamics of the soft domains is considerably slowed down, rationalizing the observed increase of the glass transition temperature.
A very similar behaviour was recently found for nanocomposites of polyurea JD-2000 filled with 1 wt% of MoS_2 nanotubes and $Mo_6S_2I_8$ nanowires.[45] Although the inorganic nanoparticles are much larger (100 nm diameter, 10μm length) and their concentration is 1-2 orders of magnitude smaller as compared to the hard nanodomains, a clear increase of T_{g1} was observed in the presence of nanoparticles, whereas T_{g2} remained constant (Fig. 13). Also in this case the increase of T_{g1} results from a slowing down of molecular motions near the nanoparticle surface, which due to an increase of the correlation length ξ extends deeply into the matrix.

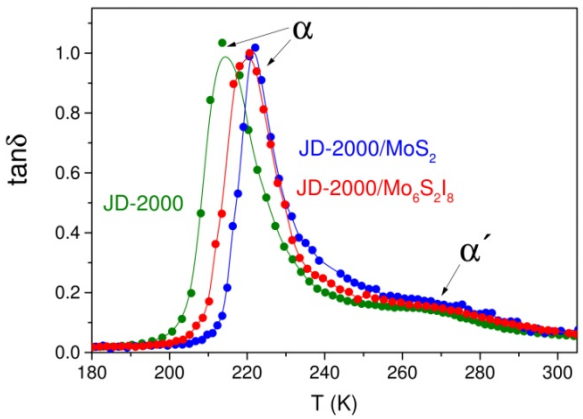

Figure 13 tanδ of pure polyurea JD-2000 compared with the nanocomposites JD-2000/MoS_2 and JD-2000/$Mo_6S_2I_8$ (1wt.% of MoS_2 and $Mo_6S_2I_8$). The measurements were performed at a frequency of 1Hz.

V Summary and conclusions

We have studied the glass transitions in microphase segregated polyurea networks by measuring the dynamic elastic susceptibility in a broad temperature range and at frequencies between 0.1 – 100 Hz. By varying the chain length l_c of the soft part of the polyurea molecules between 24.5 nm and 2.5 nm, the volume fractions ϕ_x of hard nanodomains increased from 7% to 39%, implying that the average distance *t* between the hard nanodomains decreases with decreasing chain length l_c.
Two distinct peaks in tanδ were clearly resolved at T_α and $T_{\alpha'} > T_\alpha$ for samples with 7 and 12 vol% of hard nanodomains. They were attributed to glass transitions in the soft matrix (α-peak) and at the interface between the hard nanodomains and the matrix (α'-peak), respectively. We have fitted the two tanδ peaks with two Havriliak-Negami terms and Vogel-Fulcher dependencies of the corresponding relaxation times τ_α and $\tau_{\alpha'}$. Using these fitting parameters we have determined the glass transition temperatures $T_{g1}(\phi_x)$ and $T_{g2}(\phi_x)$, corresponding to the α and the α´-process, respectively. It turns out, that T_{g1}

increases strongly with increasing volume fraction of the hard nanodomains, whereas T_{g2} remains almost constant.

The strong increase of T_{g1} with increasing ϕ_x results from the fact, that due to the observed strong increase of a dynamical correlation length ξ with $T \rightarrow T_{g1}$, the interfacially slowed down regions near the hard nanodomains extend deep into the soft matrix, and the longest relaxation time τ_α increases, resulting in an increase of the average T_{g1}. The effect increases with increasing density of the nanodomains. Molecular dynamics simulations [15,23,39,46] corroborate such a picture. On the other hand the molecules near the hard nanodomains are already strongly (chemically) attached, so that their dynamics is substantially slowed down and thus T_{g2} is not expected to be much influenced by an increase of ϕ_x, in agreement with the observations.

At the critical value of $\phi_x^c \approx 0.19$ the two glass transition temperature curves intersect, implying that at this concentration of hard nanodomains one cannot longer separate the dynamics of molecular motions close to the nanodomain interface from that of the soft matrix. At this critical concentration, the hard nanodomains start percolating and microphase segregated polyurea changes from a system of hard nanodomains embedded in a soft matrix to the opposite case of a soft polymer confined in a network of interconnected hard domains. This is also accompanied by a strong reinforcement effect, i.e. the Young´s modulus at 100 K changes from 4 GPa (for ϕ_x=0.07) to 8 GPa (for ϕ_x=0.39). The critical concentration of about 0.19 corresponds to the percolation threshold [44] of overlapping ellipsoids with an aspect ratio between 1:4 and 1:5. Of course such a simple geometrical model has at this stage to be taken with caution. E.g. if instead of rotational ellipsoids one would take overlapping spherocylinders, the observed percolation threshold [47] would imply D/L≈1:2-1:3 (D=diameter, L=length of the spherocylinder). Although such shapes of nanodomains are in reasonable agreement with some previous AFM measurements [28], more detailed investigations are needed to test these predictions which are based on a rather idealized geometrical model.

Summarizing, our findings lead to interesting insights into the two-glass transition behaviour of microphase segregated polyurea which are valid for other NPCs, too. However, as they are based on a rather macroscopic approach and phenomenological analysis they should be complemented by microscopic measurements as well as computer simulations. Detailed AFM measurements are required to reveal the morphologies of nanodomains in polyureas with different hard/soft segment ratios of the chains and to determine the corresponding average distances between the hard nanodomains as well as their exact shape. Molecular dynamics simulations of the type of Ref. 39 could help to considerably improve the quality of fitting of dynamic susceptibility data. At present we know, that in the vicinity of nanoparticles $\tau(r,T)=\tau_0(r)\exp\{\xi(r,T)\Delta(r)/T\}$ with $\tau(r\rightarrow\infty) > \tau$ (pure polymer) and we do not have a clue on the specific r-dependencies of τ_0, B and T_0 in the corresponding Vogel-Fulcher equation. Given the spatial dependence of the relaxation time – like the one shown in Fig. 11 of Ref. 39 – in an analytic form, would help to reduce the number of fitting parameters considerably and would give more physical meanings to the parameters, as compared to the rather phenomenological Havriliak-Negami fitting procedure.

In addition to the obtained fundamental insights, the present work yields results that may be also interesting from the applications point of view: The properties of polyurea can be easily tuned by varying the segmental molecular weight of polyetheramines, i.e. the volume fraction ϕ_x of hard nanodomains. The glass transition temperature increases from –75°C for ϕ_x= 0.07 to – 7°C for ϕ_x= 0.39, i.e. with decreasing molecular weight and is accompanied by a strong reinforcement effect of 100%. In principle these properties could be further improved if the density of nanodomains could be still increased. It has been shown that packing fractions of more than 0.7 can be reached for ellipsoids [48] and superellipsoids. [49] Inserting this value into Eq. (8) one obtains a theoretical glass transition temperature of 194°C. Although such high values may not be reached in practice, the polyurea elastomer ET-403 [27] with a volume fraction of ϕ_x=0.47 yields a glass transition temperature of +10°C, which is well predicted by Eq.(8) with the fitting parameters of the present work (Fig. 12).

Acknowledgements

The present work was performed in the frame of the COST Action MP0902 (COINAPO – Composites of Inorganic Nanotubes and Polymers). Financial support from the Austrian Science Fund (FWF) P23982-N20 is gratefully acknowledged.

[a]Faculty of Physics, University of Vienna, Boltzmanngasse 5, 1090 Vienna, Austria
[b]Department of Health Sciences and Technology, ETH Zurich, Institute of Food, Nutrition and Health, Food and Soft Materials Science Group, Schmelzbergstrasse 9, LFO, E29, 8092 Zurich, Switzerland

References

[1] G. Adam and J. H. Gibbs, J. Chem. Phys., 1965, **43**, 139.
[2] S. Capaccioli, G. Ruoccoand F. Zamponi, J. Phys. Chem. B, 2008, **112**, 10652.
[3] P. Debenedetti and F. H. Stillinger, Nature, 2001, **410**, 259.
[4] G. Hempel, A. Hempel, A. Hensel, C. Schick and E. Donth, J. Phys. Chem. B, 2000, **104**, 2460.
[5] S. A. Reinsberg, A. Heuer, B. Doliwa, H. Zimmermann and H. W. Spiess, J. Non-Cryst. Sol., 2002, **307-310**, 208.
[6] X.H. Qiu and M. D. Edinger, J. Phys. Chem. B, 2003, **107**, 459.
[7] L. Berthier, G. Biroli, J.-P. Bouchard, L. Cipelletti, D. ElMasri, D. L´Hote, F. Ladieu and M. Pierno, Science, 2005, **310**, 1797.
[8] C. Donati, J. F. Douglas, W. Kob, S. J. Plimpton, P. H. Poole and S. C. Glotzer, Phys. Rev. Lett., 1998, **80**, 2338.
[9] J. D. Stevenson, J. Schmalian and P. G. Wolynes, Nature Physics, 2006, **2**, 268.
[10] J. A. Forrest and J. Mattsson, Phys. Rev. E, 2000, **61**, R53.
[11] B. Jérome and J. Commandeur, Nature, 1997, **386**, 589.
[12] P. Pissis, A. Kyritsis, D. Daoukaki, G. Barut, R. Pelster and G. Nimtz, J. Phys.: Condens. Matter, 1998, **10**, 6205.
[13] C. L. Jackson and G. B. McKenna, Chem. Mater., 1996, **8**,2128.
[14] W. Schranz, M. R. Puica, J. Koppensteiner, H. Kabelka and A. V. Kityk, Europhys. Lett., 2007, **79**, 36003.
[15] P. Scheidler, W. Kob and K. Binder, Europhys. Lett., 2000, **52**, 277.
[16] P. Scheidler, W. Kob and K. Binder, Europhys. Lett., 2002, **59**, 701.
[17] O. Trofymluk, A. A. Levchenko and A. Navrotsky, J. Chem. Phys., 2005, **123**, 194509.
[18] J.-Y. Park and G. B. McKenna, Phys. Rev. B, 2000, **61**, 6667.
[19] C. LeQuellec, G. Dosseh, F. Audonnet, N. Brodie-Lindner, C. Alba-Simionesco, W. Häussler and B. Frick, Eur. Phys. J. Special Topics, 2007, **141**, 11.
[20] M. Alcoutlabi and G. B. McKenna, J. Phys.: Condens. Matter, 2005, **17**, R461.
[21] C. Alba-Simionesco, B. Coasne, G. Dosseh, G. Dudziak, K. E. Gubbins, R. Radhakrishnan and M. Sliwinska-Bartkowiak, J. Phys.: Condens. Matter, 2006, **18**, R15.
[22] H. Oh and P. F. Green, Nature Materials, 2009, **8**, 139.
[23] F. W. Starr, T. B. Schroder and S. Glotzer, Macromolecules, 2002, **35**, 4481.
[24] G. D. Smith, D. Bedrov, L. Li and O. Byutner, J. Chem. Phys., 2002, **117**, 9478.
[25] G. Tsagaropoulos and A. Eisenberg, Macromolecules, 1995, **28**, 6067.
[26] J. M. Kropka, V. Pryamitsyn and V. Ganesan, Phys. Rev. Lett., 2008, **101**, 075702.
[27] A. Sánchez-Ferrer, D. Rogez and P. Martinoty, Macromol. Chem. Phys. 2010, **211**, 1712.
[28] M. Grujicic, B. Pandurangan, T. He, B. A. Cheeseman, C.-F.Yen and C. L. Randow, Mater.Sci. Eng.A, 2010, **527**, 7741.
[29] J. Koppensteiner, W. Schranz and M. R. Puica, Phys. Rev. B, 2008, **78**, 054203.
[30] J. Koppensteiner, W. Schranz and M. A. Carpenter, Phys. Rev. B, 2010, **81**, 024202.
[31] W. Schranz, Phase Transitions, 1997,**64**, 103.
[32] J. Yi, M. C. Boyce, G. F. Lee and E. Balizer, Polymer, 2006, **47**, 319.
[33] J. A. Pathak, J. N. Twigg, K. E. Nugent, D. L. Ho, E. K. Lin, P. H. Mott, C. G. Robertson, M. K. Vukmir, T. H. Epps III and C. M. Roland, Macromol. 2008, **41**, 7543.
[34] D. Fragiadakis, R. Gamache, R. B. Bogoslovov and C. M. Roland, Polymer, 2010, **51**, 178.
[35] S. Havriliak and S. Negami, Journal of Polymer Science Part C-Polymer Symposium, 1966, 14PC, 99.
[36] F. Kremer and A. Schönhals, *Broadband dielectric spectroscopy*. Berlin; New York: Springer; 2003.
[37] N. G. McCrum, B. E. Read and G. Williams, *Anelastic and dielectric effects in polymeric solids.* New York: Dover Publications, 1991.
[38] C. Dalle-Ferrier, C. Thibierge, C. Alba-Simionesco, L. Berthier, G. Biroli, J. P. Bouchaud, F. Ladieu, D. L´Hote and G. Tarjus, Phys. Rev. E, 2007, **76**, 041510.
[39] B. A. Pazmino Betancourt, J. F. Douglas and F. W. Starr, Soft Matter, 2013, **9**, 241.
[40] P. D. Godfrey, R. D. Brown and A. N. Hunter, J. Molecular Structure, 1997, **413-414**, 405.
[41] M. Vacatello, Macromolecules, 2001, **34**, 1946.
[42] G. Tsagaropoulos and A. Eisenberg, Macromolecules, 1995, **28**, 396.
[43] H. Stutz, K.-H. Illers and J. Mertes, J. Polymer Sci.: Part B: Polymer Phys., 1990, **28**, 1483.
[44] E. J. Garboczi, K. A. Snyder, J. F. Douglas and M. F. Thorpe, Phys. Rev. E, 1995, **52**, 819.
[45] M. Reinecker, A. Fuith, V. Soprunyuk, A. Sánchez-Ferrer, A.Mrzel, R. Torre and W. Schranz, Phys. Stat. Sol. A, 2013, **210**, 2320.
[46] M. Vacatello, Macromolecules, 2001, **34**, 1946.
[47] B. Nigro, C. Grimaldi, P. Ryser, A. P. Chatterjee and P. van der Schoot, Phys. Rev. Lett., 2013, **110**, 015701.
[48] A. Donev, F. H. Stillinger, P.M. Chaikin and S. Torquato, Phys. Rev. Lett. 2004, **92**, 255506-1.
[49] G. W. Delaney and P. W. Cleary, Europhys. Lett. 2010, **89**, 34002-p1.

